Modelling particle size distribution in TELEMAC-2D with Population Balance Method

Nithin Achutha Shettigar[1], Wilhem Riom[1], Qilong Bi[1,2], Erik A. Toorman[1]
nithinachutha.shettigar@kuleuven.be
[1]: Hydraulics Laboratory, KU Leuven, Belgium
[2]: Flanders Hydraulics Research, Antwerp, Belgium

Abstract – **Modelling transport of microplastic particles in aquatic environments is challenging owing to the heterogeneity of the particles. Conventional Lagrangian and Eulerian modelling approaches come with the restriction of defining singular particle properties. Drawing inspiration from other scientific disciplines, particle heterogeneity is addressed in this work using population balance equations (PBE) with the method of moments solution. As a first step, a wide size range of microplastics is considered as internal coordinate of the number density function (NDF). The moment transport equation includes source and sink terms of erosion and deposition respectively. The method is implemented in the TELEMAC-2D and WAQTEL environments. The test case of a channel with steady state flow and erosion and deposition zones is implemented. The results of the model show physically meaningful NDFs after episodes of erosion and deposition. Further model development is planned to include the integral source and sink terms such as aggregation and breakage of flocs of microplastic and sediment particles.**

***Keywords*:** microplastics, deposition, erosion, method of moments, number density function, Telemac2D.

I. INTRODUCTION

Drastic increase in the use of plastics without proper disposal mechanisms has resulted in large quantities of plastic litter ending up in the open environment [1]. Often rivers play a crucial role in transporting plastic litter from inland to the marine environment [2]. Once disposed in the open environment, plastic litter undergoes a slow but continuous change in its size, shape and strength [3][4]. This results eventually in the apparition and multiplication of microplastic. Microplastic are generally described in the literature as plastic litters of size 5 mm or less [5]–[7]. Plastic litter of a few nanometres are also detected in many parts of the world, including on top of the glaciers [8]. This makes microplastics very challenging to track.

Modelling tools are often employed to simulate plastic litter transport pathways in the fluvial, marine and estuarian systems. Coupled hydrodynamic and Lagrangian particle tracking models can reveal the transport trajectories of plastic litter. This approach has led to claims of floating garbage patches in several parts of the world oceans [9]. However, Lagrangian models track the individual particles which requires large computational resources in order to track realistic plastic concentrations [8][9]. Moreover, the Lagrangian approach is not ideal to model the processes of plastic transport such as – deposition, erosion, aggregation, breakdown, etc. On the contrary, the Eulerian approach deals with particle mass or volumetric concentrations; therefore, modelling realistic plastic concentrations is convenient with the Eulerian approach. A major weakness of both the Lagrangian and Eulerian approach is the need for multiple classes (few tens) to address heterogeneity of plastic litter in the aquatic environment, in other word, the variety of the size, shape and density [9]. In the Eulerian approach, for each different property of the plastic, a different particle class must be defined. In order to model a wide size range – from few nanometres to few millimetres – several size classes must be defined. This requires high computational resources. A sophisticated approach exists to address this issue. Population Balance Equations (PBE) with the Method of Moments (MoM) are often used in the chemical, biochemical and industrial engineering to model the bubble size distribution in chemical applications, flocs size distribution in wastewater treatment processes, particle size distribution in the grinding process, etc [12]. In the next section the PBE approach and the mathematical model of the PBE applied to microplastic transport in aquatic environment is explained.

II. POPULATION BALANCE EQUATION

The PBE approach describes the spatial and temporal evolution of the number density function (NDF) associated with a particle population. While NDF evolves continuously due to phenomena of advection and diffusion, it can also evolve discontinuously due to aggregation, breakage, etc. [13]. In the PBE approach, a particle population is either a discrete or a continuous entity which interacts with their environment which is a continuous phase. The particle populations are defined by an array which contains both internal and external coordinates. An internal coordinate describes the properties of the particle population in the state space and an external coordinate is used to describe the particle location in the physical space [12]. The internal coordinates may include the particle's size, volume, mass or the chemical composition [14]. The mathematical expression of PBE applied to a system with a particle population in a carrier fluid consists of the Navier-Stokes equations (or other shallow water simplification) for the carrier fluid and a spatial transport equation (e.g. advection and diffusion), source terms (e.g. dissolution, deposition), integral terms

(e.g. aggregation and breakage) for the particle population [14]. In this paper, the transport of the microplastics in the liquid media is studied with a focus on the erosion and deposition as sink and source terms. Further, the size of the microplastics alone is defined as the internal coordinate of the NDF. The tested model is a 2D hydrodynamic model coupled with a PBE-based particle transport model.

The evolution of the NDF of a discrete phase of particles in a continuous medium is expressed in the following form [15]:

$$\frac{\partial hn}{\partial t} + \frac{\partial}{\partial x}(\mathrm{hU}\, n) + \frac{\partial}{\partial y}(\mathrm{hV}\, n) - \frac{\partial}{\partial x}\left(hD_x \frac{\partial n}{\partial x}\right) - \frac{\partial}{\partial y}\left(hD_y \frac{\partial n}{\partial y}\right) = S_o - S_i \quad (1)$$

where:

- $n(\xi; x, y, t)$ = number density function $[number/m^3]$ or $[1/m^3]$;
- ξ = internal coordinate of NDF e.g. particle size;
- x, y = spatial coordinate;
- U, V = depth-averaged velocities in x & y directions;
- D_x, D_y = turbulent dispersion coefficients in x & y directions;
- S_o, S_i = sink term and source term respectively e.g., aggregation, breakage, erosion, deposition, etc.

Several methods of solving PBE can be found in the literature. The class or sectional method works by discretizing the internal coordinate space into intervals (classes or sections), transforming the PBE into a set of macroscopic balance equations in the physical domain [16]. However, a large number of scalars (i.e., classes) are required to maintain reasonable accuracy [17].

In the Monte Carlo method, a finite sample of the population is used to track its evolution under the influence of growth and disintegration mechanisms with probabilities proportional to the corresponding rates [18]. However, because of the large number of scalars required, incorporating these methods into CFD codes is also computationally challenging.

An effective and more elegant solution is found through the Method of Moments (MoM). A discrete set of moment values carry the NDF information. The low order moment values are related to the mean, variance, skewness and flatness of the statistical distributions described by the NDFs [19]. In contrast to the method of classes and the Monte Carlo method, MoM is appropriate for use with CFD codes because the internal coordinates are integrated, requiring only a small number of scalars (i.e., lower order moments) at each grid point [17].

A. Method of Moments

In the case of a multivariate NDF i.e., a NDF with several internal coordinates (ξ), the k^{th} order moment (M_k) of the NDF is expressed as:

$$M_k(x, y, t) = \int_{\Omega_\xi} n(\xi; x, y, t)\, \xi_1^{k_1} \xi_2^{k_2} \dots \xi_M^{k_M}\, d\xi \quad (2)$$

where Ω_ξ represents the internal coordinate space of all the possible sizes ξ. The array $k = (k_1, k_2, \dots k_M)$ represents the order of the moment values with respect to all the internal coordinate values (ξ) taken into account [20]. In the case of single internal coordinate ξ which assumes only $\mathbb{R}^+$ (non-negative real numbers), the above moment expression reduces to:

$$M_k(x, y, t) = \int_0^{+\infty} n(\xi; x, y, t)\, \xi^k\, d\xi \quad (3)$$

The NDF transport equation (1) can be modified into a moment transport equation by multiplying it with the ξ^k and integrating over $[0, +\infty)$ [13].

$$\frac{\partial M_k}{\partial t} + \frac{\partial}{\partial x}(U\, M_k) + \frac{\partial}{\partial y}(\mathrm{V}\, M_k) - \frac{\partial}{\partial x}\left(D_x \frac{\partial M_k}{\partial x}\right) - \frac{\partial}{\partial y}\left(D_y \frac{\partial M_k}{\partial y}\right) = \int_0^{+\infty} S_o\, \xi^k\, d\xi - \int_0^{+\infty} S_i\, \xi^k\, d\xi \quad (4)$$

The solution of (4) is advantageous as the moment values hold quantities with physical meaning and therefore are measurable. M0, M1 and M2 represent the total number of particles, total length and total area respectively [21]. This overcomes difficulty of validation through the NDF, as the NDF itself is not measured in most cases but its integral quantities are measured such as total mass, total volume, etc. However, the challenge is to express the sink and source terms in moment values, which leads to closure problem.

This is addressed by means of quadrature approximation. In the Quadrature Method of Moments (QMOM), N-node Gaussian quadrature is employed to approximate the integrals in the moment transport equations for the solution of a univariate PBE. The algorithm calculates the N abscissas and N weights of the quadrature from the 2N transported moments [16]. The NDF is approximated with the discrete weighted sum of Dirac δ functions, uniquely found by means of moment inversion algorithms [13]:

$$n(\xi; x, y, t) \approx \sum_{i=1}^{N} w_i(x, y, t)\, \delta[\xi - \xi_i(x, y, t)] \quad (5)$$

which implies the moment approximation as:

$$M_k(x, y, t) \approx \sum_{i=1}^{N} w_i(x, y, t)\, \xi_i^k(x, y, t) \quad (6)$$

The abscissas $\xi_i(x, y, t)$ and the weights $w_i(x, y, t)$ are derived from the lower order moments. For a NDF approximation of order N, only the first $2N$ moments are essential [22]. In the next section, an alternative MoM-Extended Quadrature Method of Moments (EQMOM) is explained, which is the focus of the current work.

B. EQMOM procedure

In the QMOM procedure, the approximation of the NDF at certain values of the internal coordinate (ξ) can be problematic in cases where a population is diminishing continuously (for example, pure settling). An alternative MoM for such case is EQMOM which utilises continuous kernel density functions (KDF) in the place of Dirac δ functions. Several existing works have used different KDFs as applicable to the physical processes involved. Most widely reported are the Gaussian distribution with infinite support $(-\infty, \infty)$, gamma and log-normal distributions with semi-infinite positive support $[0, \infty)$ and beta distribution with finite support [0,1] [16]. The mathematical expressions of the EQMOM approximation of the NDF is:

$$n(\xi; x, y, t) \approx p_N(\xi; x, y, t) = \sum_{i=1}^{N} w_i \, \delta_\sigma(\xi, \xi_i) \tag{7}$$

where w_i and ξ_i are the weights and abscissae of the non-negative KDF. N is the number of KDFs used to approximate the NDF.

In the case where σ tends to zero, in other words the population is diminishing to few particle sizes, the KDF $\delta_\sigma(\xi, \xi_i)$ tends to a Dirac δ function, w_i are the non-negative weights and ξ_i are the respective quadrature abscissae [13]. The first step in the numerical procedure of solving EQMOM is the selection of an appropriate KDF. This choice has to be made based on the distribution of the NDF in question. From the knowledge of the size distribution of the plastic particles found in nature [7], we select the log-normal KDF. Therefore the δ function can be defined as [23]:

$$\delta_\sigma(\xi, \mu) = \frac{1}{\xi\sigma\sqrt{2\pi}} \exp\left(-\frac{(\ln\xi - \mu)^2}{2\sigma^2}\right); \xi, \sigma \in \mathbb{R}^+, \mu \in \mathbb{R} \tag{8}$$

where μ and σ are the mean and standard deviation of the natural logarithm of the log-normally distributed variable ξ. The integer moments of order k of the log-normal distribution is given by the Mellin transform [23]:

$$M_k(x, y, t) = exp\left(k\mu + \frac{k^2\sigma^2}{2}\right) \tag{9}$$

One-node case – One-node case uses one subordinate KDF to represent the whole distribution. To take bimodal (or higher) behaviour of NDF into account, using two-node (or more) is required. The one node (N=1) approximation of the NDF is the simplest case of EQMOM, which needs only the first $2N + 1 = 3$ moments to be solved [16]. In this case the approximated NDF is given as [23]:

$$\begin{aligned} n(\xi; x, y, t) \approx P_1(\xi; x, y, t) &= w_1 \delta_\sigma(\xi, \xi_1) \\ &= \frac{w_1}{\xi\sigma\sqrt{2\pi}} exp\left(-\frac{(\ln\xi - \xi_1)^2}{2\sigma^2}\right) \end{aligned} \tag{10}$$

The first three moments can be defined with (10) as follows:

$$\begin{cases} M_0 = w_1 \\ M_1 = w_1 \, e^{(\xi_1 + \sigma^2/2)} \\ M_2 = w_1 \, e^{(2\xi_1 + 2\sigma^2)} \end{cases} \tag{11}$$

Equation (12) can be analytically solved to find the values of w_1, ξ_1 and σ:

$$\begin{cases} w_1 = M_0 \\ \xi_1 = \ln\left(\dfrac{M_1^2}{M_0\sqrt{M_0 M_2}}\right) \\ \sigma = \sqrt{2\ln\left(\dfrac{\sqrt{M_0 M_2}}{M_1}\right)} \end{cases} \tag{12}$$

C. Erosion and deposition terms in the MoM framework

The fully unsteady and non-equilibrium 2D sediment transport equation is written in terms of the sediment concentration *C* as:

$$\begin{aligned} &\frac{\partial hC}{\partial t} + \frac{\partial}{\partial x}(\text{hU } C) + \frac{\partial}{\partial y}(\text{hV } C) - \\ &\frac{\partial}{\partial x}\left(hD_x \frac{\partial C}{\partial x}\right) - \frac{\partial}{\partial y}\left(hD_y \frac{\partial C}{\partial y}\right) = \\ &\text{E} - \text{D} \end{aligned} \tag{13}$$

where D = deposition rate and E = resuspension rate, both with units $[kg/m^2 s]$.

The existing sediment transport models define the erosion and deposition rates in two categories, i.e., cohesive and non-cohesive cases. A choice must be made regarding which category to be applied to the microplastic case. In order to avoid investigating through tens of empirical formulations of erosion rates under the non-cohesive category and to be able to express these rates in terms of moments of NDF, the formulation under the cohesive sediment category is adapted.

The erosion rate and deposition rate for cohesive sediments are specified as:

$$\begin{aligned} E &= \begin{cases} \text{e } C_{bed}\left(\dfrac{\tau_b}{\tau_R} - 1\right) & \text{if} \quad \tau_b > \tau_R \\ 0 & \text{if} \quad \tau_b \leq \tau_R \end{cases} \\ D &= \begin{cases} w_s \; C_{sus}\left(1 - \dfrac{\tau_b}{\tau_S}\right) & \text{if} \quad \tau_b < \tau_S \\ 0 & \text{if} \quad \tau_b \geq \tau_S \end{cases} \end{aligned} \tag{14}$$

where:

- C_{sus} = sediment concetration in suspension $[kg/m^3]$;
- C_{bed} = sediment concetration in the bed layer $[kg/m^3]$;
- w_s = sediment settling velocity $[m/s]$;
- e = erosion rate $[\text{m}/s]$;
- τ_b = bed shear stress $[\text{N}/m^2]$;
- τ_R = critical shear stress of resuspension $[\text{N}/m^2]$;
- τ_S = critical shear stress of sedimentation $[\text{N}/m^2]$;

The above formulation expressed in terms of sediment concentration needs to be adapted for the moment transport problem. The same formulation can be rewritten in terms of moment values. The moment erosion rate (E_k) and depsoition rate (D_k) are then expressed as:

$$E_k = e_\text{k} \, M_{k_{bed}}\left(\frac{\tau_b}{\tau_R} - 1\right) \tag{15}$$

$$D_k = w_{s_k} M_{k_{sus}} \left(1 - \frac{\tau_b}{\tau_S}\right)$$

where:

- $M_{k_{sus}}$, $M_{k_{bed}}$ = moment value M_k in the suspension load and bottom material respectivbely with units of 3 lower order moments being $[1/m^3], [1/m^2], [1/m]$;
- w_{s_k} = moment settling velocity $[\mathrm{m/s}]$;
- e_k = moment erosion rate $[\mathrm{m/s}]$;

Settling velocity of the k^{th} order moment w_{s_k} is expressed in the form:

$$w_{s_k} = \frac{1}{M_k} \int_0^{+\infty} \xi^k \, w_s(\xi) \, n \, d\xi \tag{16}$$

where $w_s(\xi)$ is the size dependent settling velocity e.g. Stokes equation. The above expression is essentially a weighted average of settling velocity. The erosion rate e_k is not defined in a similar integral term, instead its values are assumed irrespective of the particle size.

The resulting 2D moment transport equation is expressed as:

$$\frac{\partial h\, M_k}{\partial t} + \frac{\partial}{\partial x}(\mathrm{hU}_k\, M_k) + \frac{\partial}{\partial y}(\mathrm{hV}_k\, M_k) - \frac{\partial}{\partial x}\left(hD_x \frac{\partial M_k}{\partial x}\right) - \frac{\partial}{\partial y}\left(hD_y \frac{\partial M_k}{\partial y}\right) = E_k - D_k \tag{17}$$

III. TEST CASE: FLUME MODEL

A. Model implementation

A test case is developed in TELEMAC-2D to verify the use of PBE-MoM with erosion and deposition terms. In this regard, the modelling features available in WAQTEL – MICROPOL are utilised. WAQTEL is a water quality modelling package of the TELEMAC system (TMS) [24]. MICROPOL is a module under WAQTEL which allows modelling the evolution of the micro-pollutants e.g., heavy metals in three components of an aquatic system – water, suspended particulate matter and bottom material. Each of these components are a homogenous class. MICROPOL employs 5 tracer classes – suspended sediment (SS), bottom sediment (SF), dissolved micropollutant (C), micropollutant fraction adsorbed by suspended sediment (C_{ss}) and micropollutant fraction adsorbed by bottom sediment (C_{sf}). The SS and SF comply to the classical sedimentary physics i.e., deposition and resuspension as in case of cohesive sediments. These two processes are defined by the law of Krone and Partheniades respectively. One of the key assumptions made in MICROPOL is that SS and SF are passive tracers i.e., they do not have impact on the flow (no feedback). Therefore the bed elevation is kept unmodified during the simulation [25]. While MICROPOL is designed to be used for the micropollutant evolution, we make use of only the sediment modelling aspects to implement the PBE-MoM. The reason for this is the simplicity of the sediment transport implementation in MICROPOL and bed elevation being unmodified. At this stage, the transformation of bottom material moment values to the bed elevation is not yet determined. As a result, MICROPOL is a convenient candidate for the PBE-MoM implementation with few modifications.

As described under section II.B, in a one-node case the first three lower order moments are sufficient to reconstruct the NDF. These three moment values are treated as suspended and bottom material in MICROPOL model. In other words, the three moment values are specified for suspended class and three moments for the deposition class, resulting in a total of 6 tracers. We introduce these 6 tracers in the MICROPOL model along with the associated parameter sets. The nomenclature of the 6 moments are given in Table I. As explained in the section II.C, each of the suspended and bottom material moment values have source and sink terms i.e., erosion and deposition fluxes. The nomenclature of the parameter sets associated with erosion and deposition fluxes is given in Table II.

Table I Nomenclature of the 6 tracer introduced in MICROPOL model

Indices of unique tracers	**Description**
SS_M0, SS_M1, SS_M2	Moments M0, M1, M2 respectively in suspension load
SF_M0, SF_M1, SF_M2	Moments M0, M1, M2 respectively in bottom material

Table II Nomenclature of the parameters associated with 6 tracer introduced in MICROPOL model

Parameter	**Description**
ERO_M0, ERO_M1, ERO_M2	Erosion rate of moment M0, M1, M2 respectively
TAUS_M0, TAUS_M1, TAUS_M2	Critical shear stress of sedimentation of moment M0, M1, M2 respectively
TAUR_M0, TAUR_M1, TAUR_M2	Critical shear stress of resuspension of moment M0, M1, M2 respectively
VITCHU_M0, VITCHU_M1, VITCHU_M2	Settling velocity of moment M0, M1, M2 respectively

B. Hydrodynamic model setup

The model domain is a 50 m long and 2.5 m wide rectangular channel. The bottom elevation reduces gradually from 0 m at the flow inlet to -0.05 m at the flow outlet. The model is provided with an initial condition of 0.47 m water depth. A prescribed flowrate of 1 m^3/s is assigned at the channel inlet, while at the outlet a prescribed elevation of 0.47 m is assigned. A warming up model simulation of 500 s is carried out to create a steady state flow in the channel. The result of this simulation at t = 500 s is used as restart for the further model simulations, results of which are further presented. The further simulation and the hydrodynamic setup are given in Table III. The resulting flow pattern in the channel is a steady state flow with higher bed shear stress at the flow inlet and lower at the flow outlet. This is utilised for a further erosion and deposition behaviour criterion.

Initial moment values M0, M1, M2 are specified over the entire domain for the bottom material only. On the other hand, moment values for the suspended load are prescribed with the channel inflow from t = 0 s to t = 60 s. The values of initial bottom material moments and prescribed suspended load moments are given in Table IV. The calculation of these moment values is detailed under the following section.

Table III imulation and hydrodynamic model setup

Simulation time setup	
number of time steps	5000
time step	0.1 s
Hydrodynamic setup	
prescribed flowrates	0.0; 1.0 m^3/s (outflow boundary; inflow boundary)
prescribed elevations	0.47; 0.0 m (outflow boundary; inflow boundary)
option for liquid boundaries	2; 1 (Thompson method; strong setting)
law of bottom friction	Manning's law
friction coefficient	0.018
type of advection	1; 5; 4 (Method of characteristics for velocity; PSI distributive scheme for depth; N distributive scheme for tracer)
diffusion of tracers	$\frac{1}{h}\ div\ (hv\ \overrightarrow{grad}(T))$
Turbulence model	Constant viscosity
coefficient for diffusion of tracers	1.E-6

Table IV Initial and prescribed moment values

initial bottom material moment values	SF_M0 SF_M1 SF_M2	0.5146 $1/m^3$ 3.576E-4 $1/m^2$ 8.294E-7 1/m
prescribed suspended load moment values	SS_M0 SS_M1 SS_M2	0.5146 $1/m^3$ 3.576E-4 $1/m^2$ 8.294E-7 1/m

C. *PBE-MoM model setup*

The values of the moments M0, M1, M2 given in Table IV are estimated from the NDF associated with field measurements of microplastic particles. These field measurement are carried out under the Flemish project – PLUXIN [26]. Measurement data is collected at the Wintam area of the Scheldt river [27]. The NDF of 4,737 particles is shown in Figure 1, along with its reconstructed fit. The particles are grouped in size bins and corresponding NDF is found. Then Riemann integral with 25 bins is applied to calculate the moment value. As explained in the section II.B, the calculated moments are used to derive the parameters w_1, ξ_1 and . Next, these parameters are used to reconstruct the NDF. The mismatch between the measured and reconstructed NDF is caused by the choice of the integral approximation used to calculate the moment values. The resulting moments M0, M1, M2 are presented in Table IV. From here on, the units of M0, M1 and M2 are omitted as they remain consistent i.e., $1/m^3$, $1/m^2$ and 1/m respectively. The reconstructed NDF corresponds to mean size = 695 µm, median size = 380 µm and mode size = 114 µm.

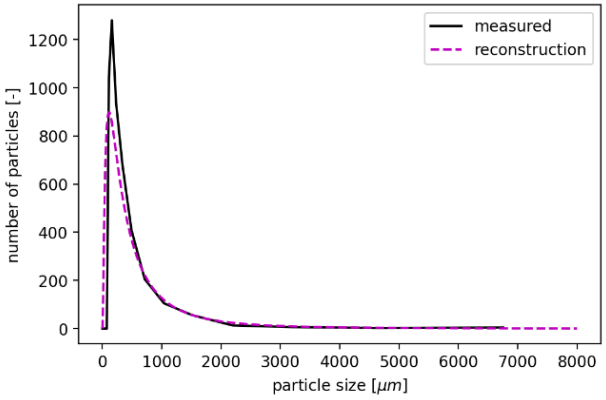

Figure 1. Measured and approximated log-normal fit of the NDF

The settling velocities w_{s_k} for the moment values are calculated as formulated in (5). The size dependent settling velocity is calculated with Stokes' equation. The initial moment values are used for the calculation of settling velocities and these settling velocities are kept constant during the simulation. As in the case of the moment value calculation, a Riemann integral with 25 bins is applied. The resulting settling velocities of the moments M0, M1, M2 are presented in Table V. In the absence of the integral size dependent formulation for the erosion rate, the initial moment values themselves are assigned to the erosion rates e_k. This implicitly allows erosion of scaled-down NDF from the bottom material at each timesteps when bed shear stress exceeds the critical shear stress of resuspension.

The critical shear stresses for resuspension and deposition are selected in order to have two distinct zones in the channel domain – an erosion zone and a deposition zone. The steady state flow allows for these zones to be static in time. The erosion zone is observed in the first 1/3rd length of the channel from the inflow boundary and the deposition zone in the last 1/3rd length of the channel (Figure 2). Further analyses on the moment and NDF evolution are carried out at two nodes roughly 14 m after the beginning of the respective zones. While the node 662 is at the end of erosion zone with a bed shear stress higher than the critical shear stress for resuspension = 2.68 N/m^2, node 840 is at the end of the deposition zone with a bed shear stress lower than the critical shear stress of deposition = 2.42 N/m^2.

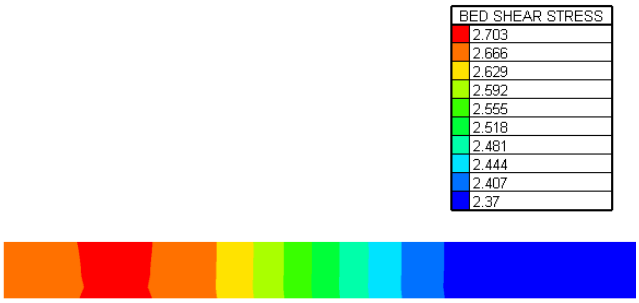

Figure 2. Bed shear stress (N/m^2) in the channel

Table V Parameters set corresponding to three moment values

PBE-MoM model parameters		
erosion rates of moments	ERO_M0	0.5146 m/s
	ERO_M1	3.576E-4 m/s
	ERO_M2	8.294E-7 m/s
settling velocity of moments	VITCHU_M0	0.083 m/s
	VITCHU_M1	0.387 m/s
	VITCHU_M2	0.756 m/s
critical shear stress of resuspension	TAUR_M0, TAUR_M1, TAUR_M2	2.68 N/m^2
critical shear stress of sedimentation	TAUS_M0, TAUS_M1, TAUS_M2	2.42 N/m^2

IV. RESULTS AND DISCUSSION

A. *Mass balance*

Firstly, the moment value conservation is checked. For this purpose, the model domain is transformed into a still basin case, by assigning all boundaries to be solid boundary. Only initial suspended load moment values (M0 = 0.5146, M1 = 3.576E-4, M2 = 8.294E-7) are imposed. This allows all the suspended moment values to be deposited as bottom material moments. The relative error after 500 s simulation is provided in Table VI. These Percentage errors show a good mass conservation of the moment values.

Table VI Mass conservation of moment values

Suspended load moments	Percentage error	Bottom material moments	Percentage error
SS_M0	-0.561E-13	SF_M0	-0.195E-10
SS_M1	0.572E-11	SF_M1	-0.138E-10
SS_M2	0.257E-8	SF_M2	-0.182E-10

B. *Moment evolution*

The moment values in suspension load as well in bottom material are further analysed over the simulation time. The evolution of moment values is shown for the two nodes with node index 662 and 840 in Figure 3.

Node 662, located at the end of the erosion zone, shows the expected behaviour in the moment values of suspension and deposition loads (Figure 3a). M0, which assumes a higher magnitude erosion rate, is intensively eroded due to the exceeded bed shear stress. However, both the M1 and M2 bed load moments do not show significant erosion as they assume erosion rates of 3 and 6 orders of magnitude less than that of M0. The eroded bed load moment is added to the suspended moments. In the M0 suspended load, we see that peak value is higher than 0.6 as compared to the prescribed M0 suspended load = 0.5146. However, this is not noticeable in the case of M1 and M2 in suspension load due to the aforementioned reasons.

Node 840, located at the end of the deposition zone, shows the deposition behaviour of the suspended load moment values (Figure 3b). It should be noted that M0 has the lowest settling velocity and M2 the highest settling velocity. This leads to M2 in the suspension load diminishing significantly in comparison to the other two moments as the bed shear stress stays below the critical shear stress for deposition. Consequently, the bed load moments also show a proportional increase in their values as suspended load moments are deposited to the bed layer. The highest gain in bed load moment is seen for M2 and the lowest one for M0.

C. *NDF evolution*

The transported moment values are transformed into a NDF in the post-processing as briefed in section II.B. The initial moment values result in a mean particle size of 695 µm, which is reflected in the bed layer NDF as shown in Figure 4a. Only a few time steps are selected for Figure 4 such that a moment set at that time at the corresponding node results in a valid NDF. The size range of the NDF are trimmed until 2000 µm, instead of full scale up to 8000 µm as meagre changes are observed at larger size range.

At node 662, located at the end of erosion zone, the bed load NDF is progressively diminishing in its peak particle number as well as the peak number is shifting towards larger particle size (Figure 4a). This is reflected in the mean particle size presented along with each subplot. This shows that the moment value erosion is reflecting the smaller particle erosion which leads to NDF skewing more towards the larger particle. It should be noted that the chosen erosion rate parameters for the moments implicitly favours the erosion of smaller particles. The suspended load NDF shows higher particle number i.e., ~1500 than the prescribed value which is ~900 (Figure 4a), which is due to the addition of eroded material to suspension. The mean size in suspended NDF is remarkably lower than the prescribed value i.e., 695 µm, also caused by the addition of eroded smaller size particles to the suspension.

At node 840, located at the end of the deposition zone, the bottom material NDF is gradually gaining the larger particle sizes reflected in the increasing number on the particles in larger size range (Figure 4b). Also, the NDF of the suspended load is gradually skewed toward the smaller size in coherence with the changes in bottom material NDF. It should be noted that the NDF of the suspended load has a mean size much lower than the prescribed value of 695 µm, as a portion of heavier particles have already settled in the deposition zone before reaching the node 840 (Figure 4b).

The NDFs of the suspended and bottom material do not show significant changes in the larger size range (>2000 µm) due to the fact that log-normal KDF is used for approximating the NDF. Log-normal distribution by its characteristics tend to zero at the larger size range. When significant changes at the larger size range is expected, more than one subordinate KDF would be required.

a)

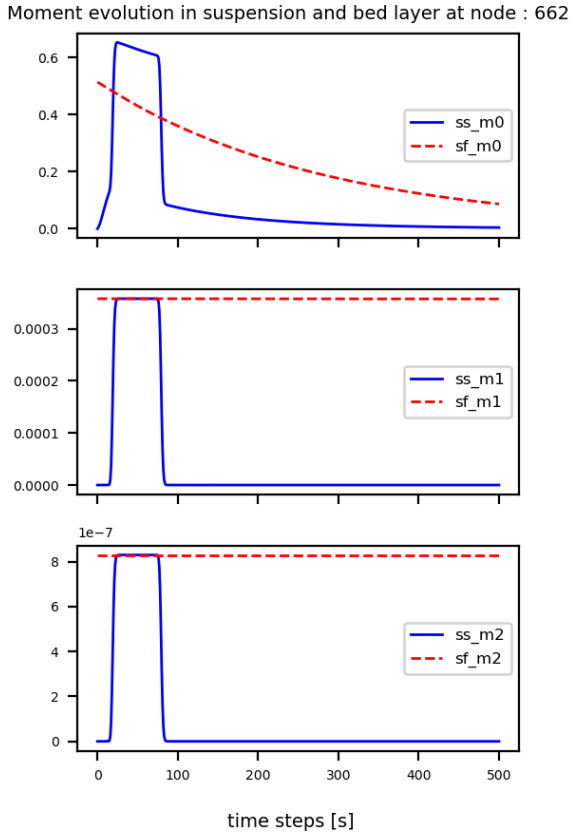

b)

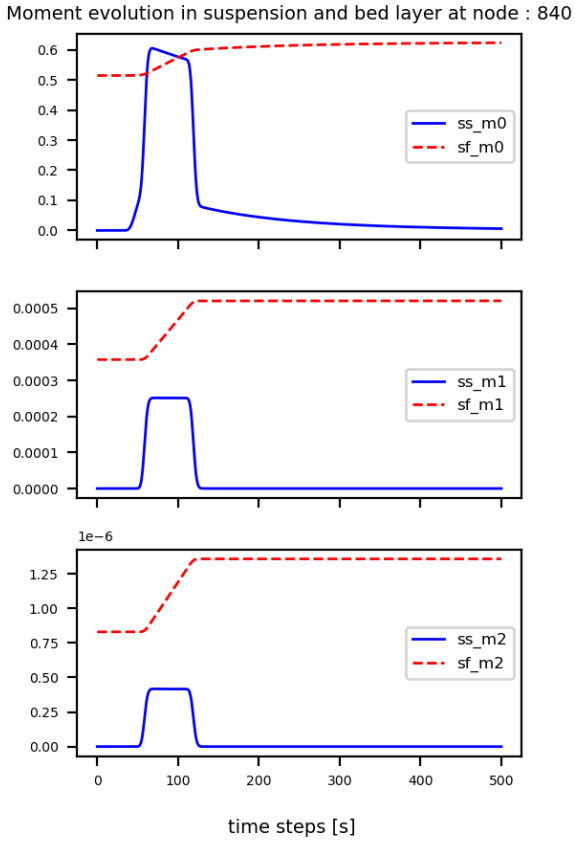

Figure 3. Moment evolution of suspended load and bottom material at two nodes a) 662 (erosion zone) and b) 840 (depostion zone). First, second and third row of plots show evolution of M0, M1 and M2 respectively.

a) b)

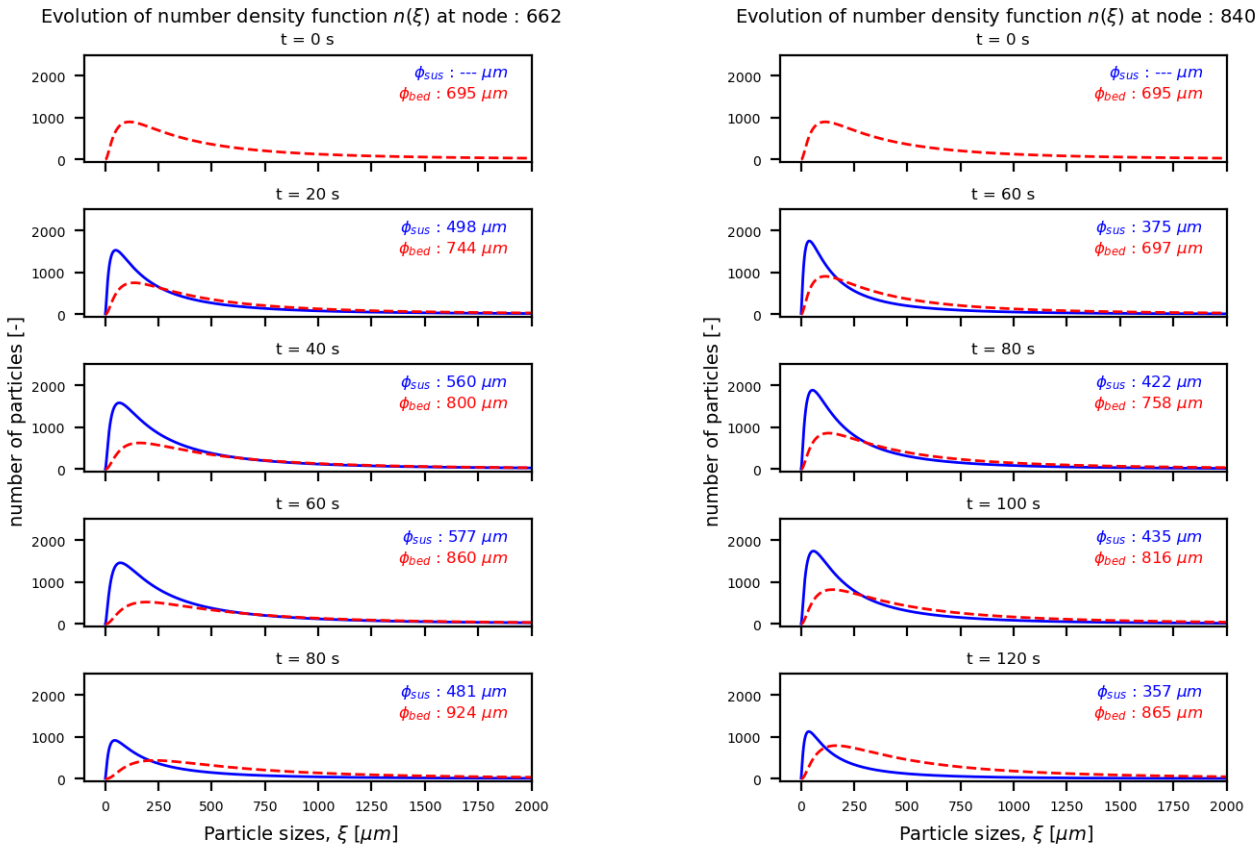

Figure 4. NDF evolution at two nodes a) 662 (erosion zone) and b) 840 (depostion zone) for selected time steps. The mean particle size of the NDF in the suspension load and bottom material are denoted as ϕ_{sus} and ϕ_{bed}.

V. CONCLUSIONS

In this study, a first attempt is made to include erosion and deposition terms in the framework of PBE-MoM. The MICROPOL module of the WAQTEL modelling package is utilised for implementing the PBE-MoM. The use of the EQMOM procedure to model the evolution of the moments and subsequently of the NDF are discussed. A procedure has been developed to determine the initial moment values as well as a post-processing technic for reconstruction of the NDF. In spite of the limited knowledge of the parameter values for erosion and deposition fluxes in MoM, physically meaningful results are obtained. The evolution of the NDF as a result of erosion and deposition are discussed and results are justified. However, the authors recognise the need for the validation of the results against measured data. In the absence of measured NDF datasets, the model needs to be first validated against concentration of suspended and deposited load. Further it is recommended that deposited bottom material moments would be transformed into mass and volumetric concentration, which can lead to the computation of bed elevation changes using the Exner equation. Apart from erosion and deposition, microplastics very likely undergo the process of flocculation with sediment and subsequent breakage of the flocs. This needs to be treated as additional source and sink terms to model the microplastic transport in aquatic environment. This would also need redefining the NDF such that both sediment and microplastic are taken into account. This is possible with multivariate NDFs and by employing more than one kernel density function to approximate the NDF. The implementation of additional source and sink terms would need reconstruction of the NDF at every time step and at every computational node. This would require efficient integral approximation methods to be implemented within the TELEMAC computation environment. Considering all the additional and unique computational requirements of PBE-MoM in TELEMAC, it is recommended to implement a standalone module.

ACKNOWLEDGEMENT

This work is carried out in the framework of the Flemish SBR PLUXIN project funded through VLAIO and the Flemish Blue Cluster (www.pluxin.be) and the EU H2020 LABPLAS project (www.LABPLAS.eu).

REFERENCES

[1] C. Lorenz *et al.*, "Spatial distribution of microplastics in sediments and surface waters of the southern North Sea," *Environ. Pollut.*, vol. 252, pp. 1719–1729, 2019, doi: 10.1016/j.envpol.2019.06.093.

[2] N. De Troyer, "Occurrence and distribution of microplastics in the Scheldt river," 2015.

[3] T. Maes *et al.*, "Microplastics baseline surveys at the water surface and in sediments of the North-East Atlantic," *Front. Mar. Sci.*, vol. 4, no. MAY, pp. 1–13, 2017, doi: 10.3389/fmars.2017.00135.

[4] M. Claessens, S. De Meester, L. Van Landuyt, K. De Clerck, and C. R. Janssen, "Occurrence and distribution of microplastics in marine sediments along the Belgian coast," *Mar. Pollut. Bull.*, vol. 62, no. 10, pp. 2199–2204, 2011, doi: 10.1016/j.marpolbul.2011.06.030.

[5] A. Malli, E. Corella-Puertas, C. Hajjar, and A. M. Boulay, "Transport mechanisms and fate of microplastics in estuarine compartments: A review," *Mar. Pollut. Bull.*, vol. 177, no. February, p. 113553, 2022, doi: 10.1016/j.marpolbul.2022.113553.

[6] H. A. Leslie, S. H. Brandsma, M. J. M. van Velzen, and A. D. Vethaak, "Microplastics en route: Field measurements in the Dutch river delta and Amsterdam canals, wastewater treatment plants, North Sea sediments and biota," *Environ. Int.*, vol. 101, pp. 133–142, 2017, doi: 10.1016/j.envint.2017.01.018.

[7] K. Aoki and R. Furue, "A model for the size distribution of marine microplastics: a statistical mechanics approach," *PLoS One*, vol. 16, no. 11, Mar. 2021, doi: 10.1371/journal.pone.0259781.

[8] P. Pastorino *et al.*, "High-mountain lakes as indicators of microplastic pollution: current and future perspectives," *Water Emerg. Contam. Nanoplastics*, vol. 1, no. 1, p. 3, Feb. 2022, doi: 10.20517/WECN.2022.01.

[9] A. S. Mountford and M. A. Morales Maqueda, "Eulerian Modeling of the Three-Dimensional Distribution of Seven Popular Microplastic Types in the Global Ocean," *J. Geophys. Res. Ocean.*, vol. 124, no. 12, pp. 8558–8573, 2019, doi: 10.1029/2019JC015050.

[10] L. Khatmullina and I. Chubarenko, "Transport of marine microplastic particles: Why is it so difficult to predict?," *Anthr. Coasts*, vol. 2, no. 1, pp. 293–305, 2019, doi: 10.1139/anc-2018-0024.

[11] F. Guerrini, L. Mari, and R. Casagrandi, "A coupled Lagrangian-Eulerian model for microplastics as vectors of contaminants applied to the Mediterranean Sea," *Environ. Res. Lett.*, vol. 17, no. 2, 2022, doi: 10.1088/1748-9326/ac4fd9.

[12] D. Ramkrishna and M. R. Singh, "Population balance modeling: Current status and future prospects," *Annu. Rev. Chem. Biomol. Eng.*, vol. 5, pp. 123–146, 2014, doi: 10.1146/annurev-chembioeng-060713-040241.

[13] A. Passalacqua, F. Laurent, E. Madadi-Kandjani, J. C. Heylmun, and R. O. Fox, "An open-source quadrature-based population balance solver for OpenFOAM," *Chem. Eng. Sci.*, vol. 176, pp. 306–318, 2018, doi: 10.1016/j.ces.2017.10.043.

[14] T. T. Nguyen, F. Laurent, R. O. Fox, and M. Massot, "Solution of population balance equations in applications with fine particles: Mathematical modeling and numerical schemes," *J. Comput. Phys.*, vol. 325, pp. 129–156, 2016, doi: 10.1016/j.jcp.2016.08.017.

[15] X. Shen, E. A. Toorman, M. Fettweis, B. J. Lee, and Q. He, "Simulating multimodal floc size distributions of suspended cohesive sediments with lognormal subordinates: Comparison with mixing jar and settling column experiments," *Coast. Eng.*, vol. 148, no. August 2018, pp. 36–48, 2019, doi: 10.1016/j.coastaleng.2019.03.002.

[16] M. Shiea, A. Buffo, M. Vanni, and D. Marchisio, "Numerical Methods for the Solution of Population Balance Equations Coupled with Computational Fluid Dynamics," *Annu. Rev. Chem. Biomol. Eng.*, vol. 11, no. 1, pp. 339–366, Jun. 2020, doi: 10.1146/annurev-chembioeng-092319-075814.

[17] D. L. Marchisio, R. D. Vigil, and R. O. Fox, "Implementation of the quadrature method of moments in CFD codes for aggregation - breakage problems," *Chem. Eng. Sci.*, vol. 58, no. 15, pp. 3337–3351, 2003, doi: 10.1016/S0009-2509(03)00211-2.

[18] K. Lee and T. Matsoukas, "Simultaneous coagulation and break-up using constant-N Monte Carlo," *Powder Technol.*, vol. 110, no. 1–2, pp. 82–89, 2000, doi: 10.1016/S0032-5910(99)00270-3.

[19] M. Pigou, J. Morchain, P. Fede, M. Penet, and G. Laronze, "New developments of the Extended Quadrature Method of Moments to solve Population Balance Equations," *J. Comput. Phys.*, vol. 365, pp. 243–268, 2018, doi: 10.1016/j.jcp.2018.03.027.

[20] A. Buffo, M. Vanni, and D. L. Marchisio, "On the implementation of moment transport equations in OpenFOAM: Boundedness and realizability," *Int. J. Multiph. Flow*, vol. 85, pp. 223–235, 2016, doi: 10.1016/j.ijmultiphaseflow.2016.06.017.

[21] X. Shen and J. P. Y. Maa, "Modeling floc size distribution of suspended cohesive sediments using quadrature method of moments," *Mar. Geol.*, vol. 359, pp. 106–119, 2015, doi: 10.1016/j.margeo.2014.11.014.

[22] D. L. Marchisio, J. T. Pikturna, R. O. Fox, R. D. Vigil, and A. A. Barresi, "Quadrature method of moments for population-balance equations," *AIChE J.*, vol. 49, no. 5, pp. 1266–1276, May 2003, doi: 10.1002/aic.690490517.

[23] E. Madadi-Kandjani and A. Passalacqua, "An extended quadrature-based moment method with log-normal kernel density functions," *Chem. Eng. Sci.*, vol. 131, pp. 323–339, 2015, doi: 10.1016/j.ces.2015.04.005.

[24] "WAQTEL user manual v8p1," 2020.

[25] "WAQTEL technical manual v8p1," 2020.

[26] "PLUXIN." https://www.pluxin.be/nl.

[27] G. Everaert *et al.*, "Plastic baseline (t0) measurement in the scope Flemish Integral Action Plan on Marine Litter (OVAM)," Flanders Marine Institute, Ostend, Belgium, 2020.